Journal of Pharmaceutical & Biomedical Analysis
Vol. 4, No. 4, pp. 461–474, 1986
Printed in Great Britain

0731–7085/86 $3.00 + 0.00
Pergamon Journals Ltd.

Binding isotherms by continuous-flow dynamic dialysis*

NEIL ARTHUR SPARROW,† LESLIE GLASSER‡, DAVID GLASSER§ and ALLAN EDWARD RUSSELL

Leather Industries Resarch Institute, Rhodes University, P.O. Box 185, Grahamstown 6140, South Africa.

Abstract: The classical dynamic dialysis technique for the determination of a protein–ligand binding isotherm has been modified by the introduction of a flow cell in which the dialysate on the sink side of the membrane is continuously eluted with a constant flow of eluting buffer and its ligand concentration measured. This new experimental method is termed continuous-flow dynamic dialysis (CFDD).

A transfer function procedure for extracting the binding isotherm from the dialysis data is described. This is a more general technique (requiring only a verifiable assumption of linearity) than that previously used, in which the system was modelled using Fick's first law and which relied on the establishment of quasi-steady state conditions across the membrane.

The present analysis uses the Laplace transform to effect deconvolution of the impulse response function of the cell from the dialysis data and, using a Fourier series approach, directly yields numerical data representing the free ligand concentration in equilibrium with the protein–ligand complex. The protein–ligand binding isotherm is obtained in parametric form, with time as the parameter.

Keywords: *Binding isotherms; Laplace transforms; continuous flow analysis; bovine serum albumin; phenol red.*

Introduction

Dialysis methods for the investigation of protein–ligand interactions have undergone considerable refinement since the original equilibrium dialysis method was reported [1]. In order to overcome several of the disadvantages of the equilibrium method, various dynamic dialysis methods have evolved [2–9]. These methods, in general, utilize Fick's first law of diffusion to establish the concentration of unbound ligand which is in equilibrium with the protein–ligand complex. This involves the measurement of the

*Supported by grants from the S.A. Meat Board, the Hide and Skin Industry, and the S.A. Council for Scientific and Industrial Research.

†Present address: School of Pharmaceutical Sciences, Rhodes University, Grahamstown 6140, South Africa. To whom correspondence should be addressed.

‡Present address: Department of Chemistry, University of the Witwatersrand, Johannesburg 2001, South Africa.

§Present address: Department of Chemical Engineering, University of the Witwatersrand, Johannesburg 2001, South Africa.

instantaneous rate of ligand diffusion. Consequently, the dialysis data are usually fitted by regression procedures to an empirical function in time, which is then differentiated analytically. The selection of an appropriate function to describe the dialysis process, in turn, depends on the prior choice of a particular binding model [10].

In a previous paper [11], a continuous-flow dynamic dialysis method was reported. This method uses a flow cell from which the dialysate on the sink side of the membrane is continuously eluted with a constant flow of eluting buffer. The ligand concentration in the eluate is automatically monitored to obtain values for the instantaneous rate of ligand diffusion from which a protein–ligand binding isotherm can be determined. This method offers several advantages over earlier methods.

The analysis of the data was based on assuming that the diffusion of the ligand through the membrane could be described by Fick's first law of diffusion. While this method appeared to give good results after establishment of a quasi-steady state across the membrane, the early part of the curves was not adequately described and, in addition, numerical differentiation of the data was required.

The previous results are now re-analysed using a more general method, based on the transfer function approach, where the assumptions required in order to get the desired isotherms are kept to a minimum. This approach requires transformation of the experimental data from the time to the frequency domain. Although there are many advantages of this procedure, which will appear in the course of the presentation, it should be pointed out that certain disadvantages do accrue; specifically, discontinuities in the data introduce problems and truncation of infinite series is necessary. An approach to handling these problems will be discussed below.

Experimental

Apparatus

The essential features of the dialysis cell and a schematic diagram of the apparatus are shown in Figs 1a and 1b, respectively. The sample is introduced into the top chamber by means of a gas-tight syringe. The eluting buffer passes first through the lower compartment at a constant rate and then through a spectrophotometer flow-cell, where the ligand concentration is automatically monitored at convenient regularly-spaced time intervals and recorded in a computer-readable format. Temperature control is achieved by immersing the dialysis cell into a Colora constant temperature bath used in conjunction with a Colora–Tauchkühler cold finger system to provide a heat sink.

Materials

Bovine serum albumin (BSA) fraction V was supplied by E. Merck (Darmstadt). Phenol red (ϵ = 10 800 l mol^{-1} cm^{-1} at λ = 340 nm) was recrystallized by acidifying a solution in sodium bicarbonate with hydrochloric acid. The semi-permeable dialysis membrane consisted of Visking cellulose (6.3 μm thickness, 4465-A2, supplied by Union Carbide) which had a specified average pore diameter of 40 nm. Phenol red–BSA binding studies were carried out in a 0.05 M sodium phosphate buffer pH 7.0 at 25°C. The binding studies were carried out over a phenol red concentration range 0.15 $\times$ 10^{-4} to 0.2 $\times$ 10^{-2} M. The BSA concentration was standardized to a value of 0.4 $\times$ 10^{-4} M, based on $A^{1\%}_{1\,cm}$ = 6.6 at a wavelength of 260 nm. Eluting buffer flow rates were within the range 0.15 $\times$ 10^{-2} to 0.75 $\times$ 10^{-2} cm^{3}s^{-1}. The contents of the sink and sample compartments were stirred at 100 rpm.

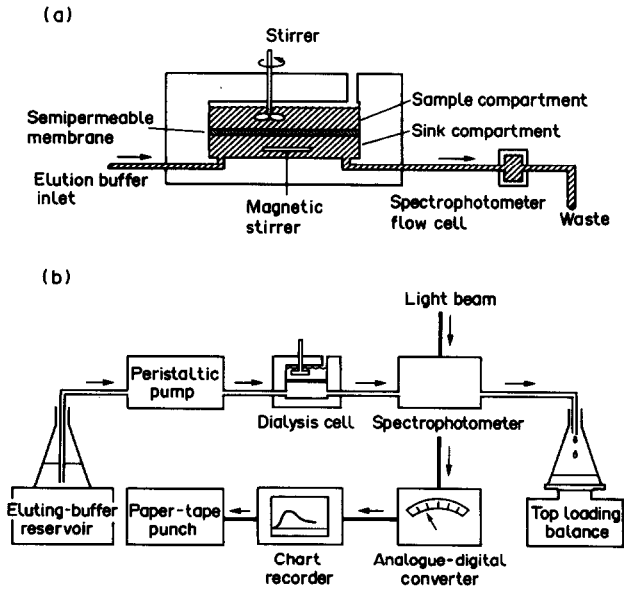

Figure 1
(a) The continuous-flow dynamic dialysis cell. (b) Schematic diagram of the continuous-flow dynamic dialysis apparatus.

Analysis

An overall mass balance for the system when no protein is present may be written:

$$v_1C_1(\mathrm{O}) - v_1C_1(t) = v_2C_2(t) + F\int_o^t C_2(\tau)\,\mathrm{d}\tau \qquad (1)$$

where the symbols have the following meanings:

$C_1(t)$	is the free ligand concentration in the sample compartment (compartment 1);
$C_2(t)$	is the ligand concentration in the sink compartment (compartment 2);
F	is the constant eluting buffer flow rate;
v_1	is the sample volume;
v_2	is the sink compartment volume;
$v_1C_1(\mathrm{O})$	is the initial quantity of ligand added.

The left-hand difference represents the quantity of ligand which has diffused from the sample compartment. The terms on the right represent, in sequence, ligand in the sink compartment, and ligand which has been transported away.

The equivalent mass balance when protein is present is:

$$v_1C_1^*(\mathrm{O}) - v_1C_1^*(t) - pC_3^*(t) = v_2C_2^*(t) + F\int_o^t C_2^*(\tau)\,\mathrm{d}\tau \qquad (2)$$

where the asterisk superscript refers to a measurement in which protein is present;

p is the number of moles of protein;

$C_3^*(t)$ is the amount of bound ligand per mole of protein.

It is an implicit assumption of this mass balance that there is negligible hold-up of ligand by the membrane. If there is a linear membrane dialysis process it may be described by a transfer function [12].

Thus:

$$C_2(t) = \int_o^t C_1(t - \tau).I(\tau)d\tau \tag{3}$$

where $I(\tau)$ is the impulse response of the membrane. The same relation must hold for the variables with the asterisk since it is assumed that the presence of the protein does not affect the membrane process for the free ligand: i.e.

$$C_2^*(t) = \int_o^t C_1^*(t - \tau).I(\tau)d\tau. \tag{4}$$

In order to continue the analysis, each of these equations is Laplace transformed, where a tilde ($\tilde{}$) denotes a transformed variable, a function of s, as defined in equation (5) below:

$$\tilde{C}_j \equiv \tilde{C}_j(s) = \int_o^\infty \exp(-s\tau)C_j(\tau)d\tau \qquad j = 1,2,3 \tag{5}$$

giving for equation (1):

$$\frac{v_1C_1(O)}{s} - v_1\tilde{C}_1 = v_2\tilde{C}_2 + \frac{F}{s}\tilde{C}_2 \tag{6}$$

where

$$\tilde{C}_2 = \tilde{I}.\tilde{C}_1 \tag{7}$$

and for equation (2):

$$\frac{v_1C_1^*(O)}{s} - v_1\tilde{C}_1^* - p\tilde{C}_3^* = v_2\tilde{C}_2^* + \frac{F\tilde{C}_2^*}{s} \tag{8}$$

where

$$\tilde{C}_2^* = \tilde{I}.\tilde{C}_1^*. \tag{9}$$

When carrying out an experiment with no protein present, it is possible, in principle, to evaluate the transfer function, $\tilde{I}$, in terms of the transformed measured variable, $\tilde{C}_2$, using equation (6):

$$\begin{aligned} I &= \tilde{C}_2/\tilde{C}_1 \\ &= sv_1\tilde{C}_2/\{v_1C_1(O) - \tilde{C}_2[v_2s + F]\}. \end{aligned} \tag{10}$$

This result can now be used with equations (8) and (9) to get a parametric representation

of the Laplace transform of the isotherm in terms of the Laplace transform of the measured variable for the protein-containing case, $\tilde{C}_2^*$.

$$\tilde{C}_1^* = \frac{\tilde{C}_2^*}{sv_1\tilde{C}_2}\{v_1C_1(O) - \tilde{C}_2[v_2s + F]\} \tag{11}$$

and

$$\tilde{C}_3^* = \frac{v_1C_1^*(O)}{p\,s} - \frac{\tilde{C}_2^*}{p}\left\{\frac{v_1C_1(O) - \tilde{C}_2(v_2s + F)}{s\tilde{C}_2} + v_2 + F/s\right\}. \tag{12}$$

Fourier series analysis

The experimental measurements of $C_2(t)$ and $C_2^*(t)$ (Fig. 2) need to be used to obtain the required isotherm.

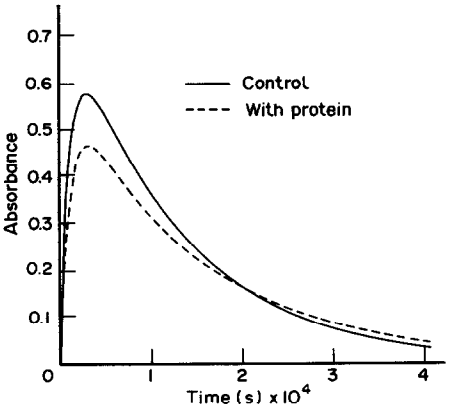

Figure 2
Experimentally obtained elution profiles for a phenol red solution and a phenol red–BSA mixture, monitored spectrophotometrically at 269 nm.

Let (as in Greenberg [13] and Karstaedt *et al.*; unpublished results):

$$s = \alpha + i\omega \tag{13}$$

where $\alpha > \alpha_o$, the largest real part of a pole of the Laplace transfer in the complex plane.

Then equation (5) becomes:

$$\tilde{C}_j(\alpha + i\omega) = \int_o^\infty \exp(-\alpha\tau)\, C_j(\tau)\, \{\cos\omega\tau - i\sin\omega\tau\}d\tau. \tag{14}$$

This integral may be approximated as closely as required by choosing a sufficiently large time limit ($2T$) for a given α, because $C_j(t) \to 0$ as $t \to \infty$, i.e.

$$\tilde{C}_j(\alpha + i\omega) \simeq \int_o^{2T} \exp(-\alpha\tau)C_j(\tau)\, \{\cos\omega\tau - i\sin\omega\tau\}d\tau \tag{15}$$

$$j = 1,2,3$$

Defining

$$g_j(t) = \exp(-\alpha t)\ C_j(t) \tag{16}$$

then (since g satisfies the Dirichlet conditions) g is approximated by a Fourier series:

$$g_j(t) = a_{jo}/2 + \sum_{m=1}^{\infty} [a_{jm} \cos(m\pi t/T) + b_{jm}\sin(m\pi t/T)]. \tag{17}$$

Now let ω take on the successive values:

$$\omega = m\pi/T \qquad m = 0,1 \ldots,\infty \tag{18}$$

and by evaluating the integral

$$\begin{aligned} &\int_O^{2T} g_j(\pi)e^{-i\omega\tau}d\tau \\ &= \int_O^{2T} e^{-\omega\tau} \left\{a_{jo}/2 + \sum_{m=1}^{\infty} [a_{jm} \cos(m\pi\tau/T) + b_{jm} \sin(m\pi\tau/T)]\right\} d\tau \end{aligned} \tag{19}$$

which because of the orthogonality of the sin and cos terms reduces to:

$$\begin{aligned} &\tilde{g}_j(\alpha + im\pi/T) = T(a_{jm} - ib_{jm}) \\ &\qquad\qquad\qquad\qquad\qquad\qquad\qquad\qquad\qquad\qquad j = 1,2,3 \\ &\qquad\qquad\qquad\qquad\qquad\qquad\qquad\qquad\qquad\qquad m = 1,\ldots,\infty \end{aligned} \tag{20}$$

therefore

$$a_{jm} = 1/T\ \mathrm{Re}[\tilde{g}_j(\alpha + im\pi/T)]; \tag{21a}$$

$$b_{jm} = -1/T\ \mathrm{Im}[\tilde{g}_j(\alpha + im\pi/T)]; \tag{21b}$$

and

$$a_{jo} = 1/T\ \tilde{g}_j(\alpha) \tag{21c}$$

also, by the Euler–Fourier formulae [14];

$$a_{jm} = 1/T \int_o^{2T} \exp(-\alpha\tau) C_j(\tau) \cos(m\pi\tau/T) d\tau \qquad m = 0,1 \ldots,\infty \tag{22a}$$

$$b_{jm} = 1/T \int_o^{2T} \exp(-\alpha\tau) C_j(\tau) \cos(m\pi\tau/T) d\tau \qquad m = 0,1 \ldots,\infty. \tag{22b}$$

It is now possible to evaluate a_{2m}, b_{2m}, a^*_{2m}, b^*_{2m}, from the experimental data of $C_2(t)$ and $C_2{}^*(t)$ by using the appropriate equation (22).

By substituting these values for the as and bs in equations (11) and (12), the following equations are obtained:

$$T(a^*_{1m} - ib^*_{1m}) = \frac{T(a^*_{2}m - ib^*_{2m})}{(\alpha + im\pi/T)\, v_1 T(a_{2m} - ib_{2m})} \{v_1 C_1(O) - T\{a_{2m} - ib_{2m}\}\, [v_2(\alpha + im\pi/T) + F]\} \tag{23}$$

and

$$T(a^*_{3m} - ib^*_{3m}) = \frac{v_1 C^*_1(O)}{p(\alpha + im\pi/T)} - \frac{T(a^*_{2m} - ib^*_{2m})}{p} \left\{\frac{v_1 C_1(O) - T(a_{2m} - ib_{2m})\, [v_2(\alpha + im\pi/T) + F]}{(\alpha + im\pi/T)\, T(a_{2m} - ib_{2m})} + v_2 + \frac{F}{(\alpha + im\pi/T)}\right\} \qquad m = 1,2, \ldots,\infty. \tag{24}$$

By taking real and imaginary parts of the right-hand sides of each of these equations, in which there are only known quantities, it is possible to evaluate a^*_{1m}, b^*_{1m}, a^*_{3m}, b^*_{3m}; $m = 1, \ldots,\infty$.

The values a^*_{1o} and a^*_{3o} may also be evaluated from the same equation with $b^*_{1o} = b^*_{3o} = 0$, provided that $\alpha > 0$. Thus all the Fourier series coefficients which are required in order to obtain the parametric representation of the isotherm are calculated.

$$C^*_1(t) = \exp(\alpha t) \left\{a^*_{1o}/2 + \sum_{m=1}^{\infty} [a^*_{1m} \cos(m\pi t/T) + b^*_{1m} \sin(m\pi t/T)]\right\} \tag{25a}$$

$$C^*_3(t) = \exp(\alpha t) \left\{a^*_{3o}/2 + \sum_{m=1}^{\infty} [a^*_{3m} \cos(m\pi t/T) + b^*_{3m} \sin(m\pi t/T)]\right\} \tag{25b}$$

for $0 \leqslant t \leqslant 2T$.

Analysis of experimental data

If a few experiments are performed without proteins, with different initial concentrations of ligand, $C_1^k(O)$, then it is possible to test the assumption of linearity since, if it is valid, all of the normalized curves $FC_2^k(t)/v_1 C_1^k(O)$ should be coincident. This is shown in Fig. 3a, where it can be seen that linearity is accurately obeyed over a four-fold range of initial concentrations.

Because of the lengthy duration of the experiments ($\simeq$7 h), it may not be convenient to continue taking measurements until the value of the concentration reaches a negligible level. In order to overcome this problem, a value of α may be chosen that is sufficiently

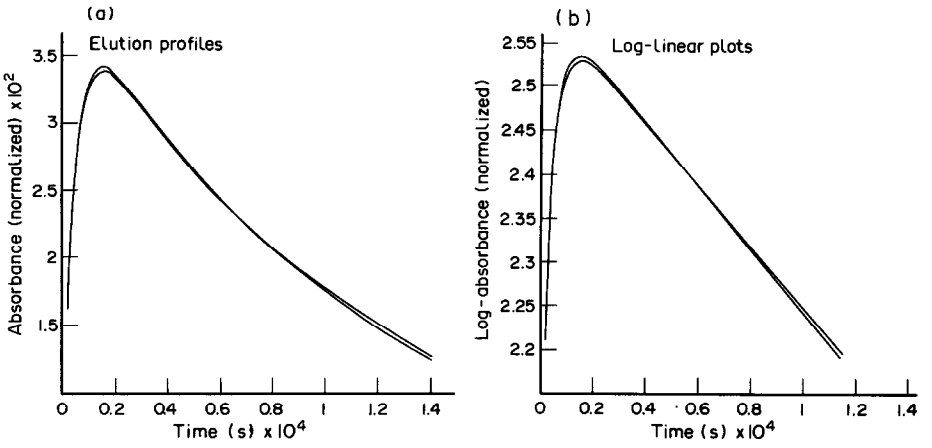

Figure 3
(a) Verification of the assumption of linearity, as shown by the coincidence of the elution profiles normalized by multiplication by $F/(\nu_1 C_1{}^K(O))$. Initial phenol red concentrations 0.5×10^{-4} M; 1.0×10^{-4} M; 1.5×10^{-4} M. (b) Log–linear plots of the normalized elution profiles.

large that the tail of the curve will fade rapidly away in order to make the approximation in equation (15) valid. This is, however, done only at the expense of also de-emphasizing the later experimental points. It was considered that the problem could be approached in another way. If the elution profiles are plotted as the logarithm of the absorbance versus time (Fig. 3b), it is clear from the linearity that the tail may be fitted by a single exponential. By using an exponential to extend the data analytically to infinity, it was shown that the correct area under the curve was obtained, viz. $(\nu_1 C_1(O)/F)$. Thus, the curve may be extended exponentially from the final experimental point T' to some arbitrary time $2T$, at which stage the value of the tail is negligible. (The error incurred may be calculated from the known value of the integral.)

For experiments in which a protein is present in the sample compartment, an equivalent analysis may be performed, but there is no good reason in this case to assume an exponential tail. (Indeed, this is most unlikely.) It is the case that the tail does appear to be fitted by an exponential, but such extension leads to a slightly incorrect area under the curve. For the sake of the mass balance, it is more important to obtain the correct area. Hence, it was decided to fit an exponential to the tail, in which constants were used to yield the correct total area according to the quantity of ligand originally introduced into the dialysis cell.

Verification of the method

In order to test the procedure and its accuracy, the analysis was first performed on a set of synthetic data, where all the model constants were known.

The protein–ligand binding isotherms were generated by means of the two-site Scatchard binding model:

$$C^*_3 = \sum_{n=1}^{m} n_i k_i C^*_1/(1 + k_i C^*_1) \qquad (26)$$

(where n_i is the number of binding sites in each class of binding site, m is the number of classes of binding sites, two in the present case, and k_i is the corresponding protein–ligand association constant for each class of binding site). Values for the binding parameters used to generate the isotherms are [15]

$$n_1 = 1,\ k_1 = 1.1 \times 10^5;\ n_2 = 6,\ k_2 = 1.2 \times 10^3.$$

For the dialysis membrane the model was taken to be that used in a previous paper [11] and the value of the membrane permeation constant used was $1.0 \times 10^{-4}\text{cm}^3\text{s}^{-1}$.

Elution profiles which simulate non-protein and protein dialysis experiments for a phenol red–BSA system were generated by computer, by solving the assumed system differential equations using a fourth order Runge–Kutta algorithm over the time interval $t = 0$ to $T' = 2.8 \times 10^4$ s (corresponding to 875 data observations at 32 s intervals). The data set was extended over an interval from $T' = 2.8 \times 10^4$ to $2T = 1.5 \times 10^5$ s, by means of a monoexponential function with values for the parameters chosen to make the function continuous with the elution profile and, as mentioned above, to obtain the correct area under the curve.

In order to perform the analysis, a value of $\alpha > 0$ (in order to be to the right of a pole at zero) has to be chosen. It should not be chosen too large, as this causes loss of accuracy by de-emphasizing the later experimental points. A value of one-tenth of the exponential constant required to fit the tail of the non-protein case was chosen. Of course, this value must be the same for both the protein and non-protein cases.

Finally, in order to perform the analysis the number of terms to be used in the Fourier series has to be chosen, since it is obviously not possible to sum to infinity. Now, because all the functions in the system obey the Dirichlet conditions [12], the Fourier coefficients will tend to zero for large values of m. However, because of experimental noise, the power $(\sqrt{a_m^2 + b_m^2})$ as a function of m tends to a constant value for large values of m ('the rectangle of noise'). At this point, it is not worth continuing to evaluate more terms since only noise is being fitted. Though this limit was approached for fewer terms, a value of $N = 100$ was used for all the work in this paper, to ensure that no true information was arbitrarily excluded.

The computer language used (FORTRAN) could perform complex arithmetic, and therefore could establish the real and imaginary parts of equations (11) and (12) without algebraic manipulation.

By using the previous analysis, it is possible to regenerate not only the binding isotherms from the computer-generated results but also $C_1(t)$, $C_1^*(t)$, and the total ligand concentration in the sample compartment: i.e.

$$C_1'(t) = C_1^*(t) + \{p/v_1\}C_3^*(t).$$

The theoretical curves, as well as the regenerated curves, were produced and compared (Fig. 4). Apart from a prominent regular oscillation, the fit of the regenerated to the theoretical curve was good. Now, it is well known that when Fourier series are fitted to functions with discontinuities, there occur oscillations associated with the Gibbs phenomenon [14]. For all three of these curves, there is a jump from zero to the initial concentration, thus causing the oscillations in the regenerated Fourier series.

Lanczos has described a method of σ factors to smooth out these oscillations [16] and, although this does damp out the oscillations, there remains some overshoot at $t = 0$, with

damped oscillations. Another procedure to eliminate the initial step, and hence these oscillations, is that of Krylov [17].

It is known that, for a function with a discontinuity at zero, the Fourier coefficients of the sine must converge [14], like $1/m$. By plotting a_m vs $1/m$, the value of the slope for large m can be established experimentally, say d. Now, it is well known that:

$$d \sum_{m=1}^{\infty} \frac{1}{m} \sin \frac{m\pi t}{T} = \frac{d\pi}{2T} (2T - t) \qquad 0 \leq t \leq 2T. \tag{27}$$

Thus, by calculating this sum to infinity, the equations for C_1, $C_1{}^*$, $C_1{}^t$, respectively can be rewritten, in the form:

$$C(t) = \sum_{m=1}^{N} (a_m - \frac{d}{m}) \sin \frac{(m\pi t)}{T} + b_m \sin \frac{(m\pi t)}{T} + \frac{d\pi}{2T} (2T - t) \tag{28}$$

where the Fourier series from equation (27) have been subtracted, term by term, and then later added as its analytical equivalent. In essence, an analytical sum to infinity has been performed on the slowly convergent part of the function, leaving a remainder term, which is more rapidly convergent-summed to N.

Figures 5a and 5b show the theoretical and regenerated curves after application of the Krylov ramp subtraction technique to remove the Gibbs phenomenon, while Fig. 5c shows the regenerated binding isotherm compared with the original. It can be seen that the technique has worked well and has been able to give a fairly accurate representation of all the data using only the output curves, without any detailed model except for the assumption of linearity and of the absence of any hold-up in the membrane.

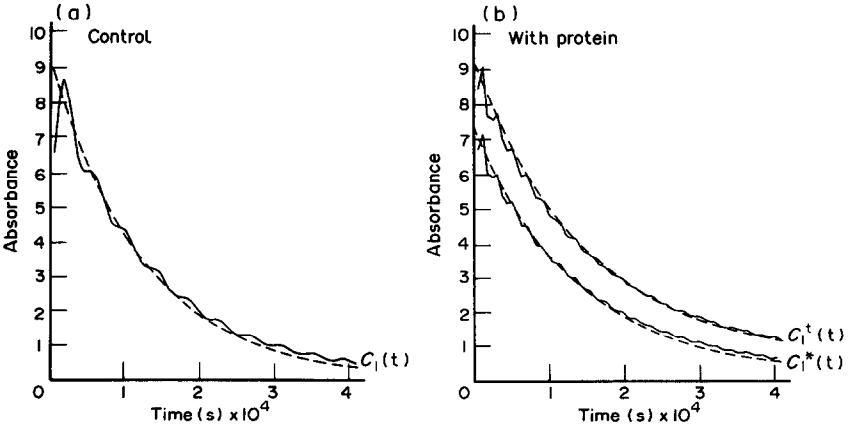

Figure 4
Sample compartment ligand concentration curves. – – – Theoretical curves. ——— Curves generated by means of the transfer function.

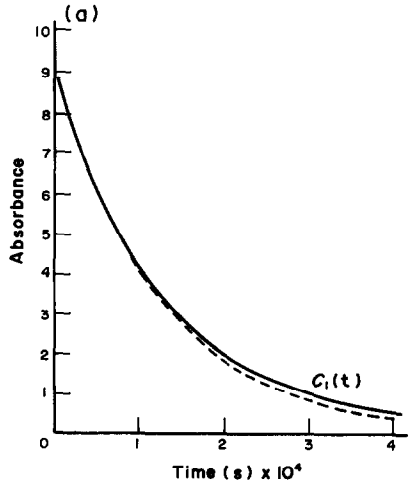

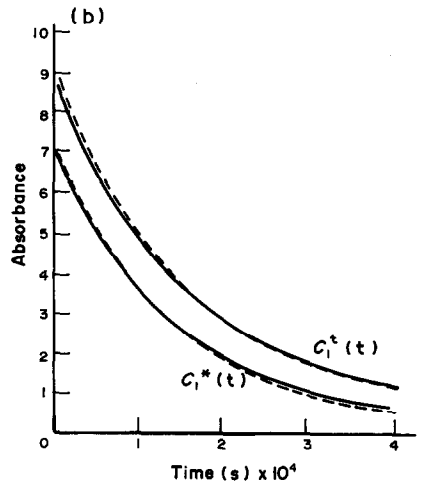

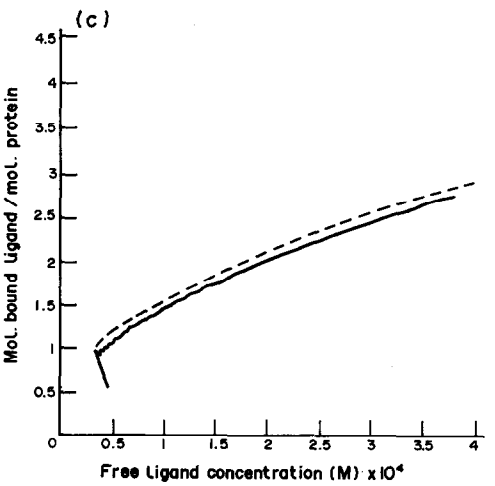

Figure 5
Sample compartment ligand concentration curves and binding Isotherms after smoothing by the Krylov method. - - - Theoretical curves. ——— Curves generated by means of the transfer function. (A) Control (no protein); (B) sample compartment ligand concentration in the presence of protein; (C) protein–ligand binding isotherms.

Figure 6a shows a comparison of the phenol red–BSA binding isotherms obtained experimentally, using the continuous flow dynamic dialysis method, with isotherms generated by equation (26) using values for binding parameters reported by other investigators. The isotherm obtained by the continuous-flow dynamic dialysis method is a composite of separate dialysis experiments over the concentration ranges listed in Table 1.

The experimental binding isotherms shown in Fig. 6a were obtained using the permeation constant method of analysis [11]. Values for binding parameters, derived from the binding isotherm, are given in Table 2. These parameters were obtained by fitting the isotherm to a two-site Scatchard model using the STEPIT least squares regression program [19]. Binding parameters recalculated from data reported by other investigators are also tabulated. The experimentally determined binding isotherms extracted from the same elution profile data sets (initial phenol red concentration 0.11×10^{-2} M; BSA concentration 5.0×10^{-5} M) by the permeation constant method and by the transfer function method are shown for comparison in Fig. 6b (i) and (ii), respectively.

Table 1
Ligand concentration ranges covered in individual dialysis experiments to prepare the composite binding isotherm

Experiment number	Initial ligand concentration (mol l^{-1})	Final ligand concentration (mol l^{-1})
1	2.33×10^{-3}	7.48×10^{-4}
2	8.31×10^{-4}	2.74×10^{-4}
3	2.87×10^{-4}	1.10×10^{-4}
4	1.61×10^{-4}	4.22×10^{-5}
5	4.20×10^{-5}	2.15×10^{-5}

Table 2
Binding parameters for the phenol red–BSA interactions at 25°C and their approximate standard errors

Method	No. of data points	n_1*	k_1 litre mol^{-1}	n_2*	k_2 litre mol^{-1}
Difference spectroscopy†	12	1	$(0.92 \pm 2.7) \times 10^5$	6	$(1.29 \pm 0.47) \times 10^3$
Dynamic dialysis‡	38	1	$(3.64 \pm 5.8) \times 10^5$	6	$(1.52 \pm 0.37) \times 10^3$
Dynamic dialysis§	32	1	$(0.57 \pm 1.1) \times 10^5$	6	$(2.05 \pm 0.42) \times 10^3$
Continuous-flow Dynamic dialysis‖	>500	1	$(0.56 \pm 0.08) \times 10^5$	6	$(1.37 \pm 0.02) \times 10^3$

*Constrained to integer values.
†Data from Rodkey [15]; parameters recalculated, using STEPIT, in order to estimate standard errors.
‡Data from Meyer and Guttman [3] see footnote †.
§Data from Kanfer [18] see footnote †.
‖Data from Sparrow *et al.* [11]; 15 points running smooth used to obtain the derivative.

Sources of error

The analysis reported above may be affected by errors of three kinds: random noise in the experimental data, systematic error, and numerical error. Random experimental noise is, fortunately, automatically smoothed by the process of Fourier analysis which necessarily omits the higher-frequency, noise-affected coefficients.

The assumption that the tail of the curve from T' to $2T$ can be modelled by a single fitted exponential will also lead to error, but this is limited to the contribution of the tail to the integrations in equations (22). Thus it is important to proceed with data capture to a point at which the elution profile is sufficiently close to zero. It is also necessary to choose $2T$ such that the exponential has approached zero sufficiently closely to make the approximation in equation (15) valid.

Systematic error, such as inadequacies in the model, will cause the final isotherm that is generated to deviate from experimental isotherms derived by more conventional methods; adequate coincidence of such isotherms are demonstrated in Fig. 6b.

Numerical error will occur if equations (23) and (24) either have denominators which tend to zero or if small differences are generated in the numerators. The former is unlikely since the denominators, when the expression is separated into real and imaginary parts, contain terms of the form $(a_n^2 + b_n^2)$. These are 'power' terms and cannot drop to near zero in this experimental situation. Small differences are, however, possible. In order to avoid this and so obtain meaningful results, it is necessary that there is a significant difference between the elution curves for protein and control. This should be confirmed, perhaps by checking that the signal-to-noise ratio (i.e. the standard deviation) of the difference signal between control and protein elution profiles is sufficiently large relative to the signal-to-noise ratio of the elution profiles themselves.

Discussion

It can be seen from Figs 6a and 6b that the phenol red–BSA binding isotherm obtained by the continuous-flow dynamic dialysis technique is consistent with the isotherms obtained by other techniques. It should be noted that the pair of curves 1 and 2 derive from a dynamic dialysis procedure which neglects back-diffusion, while the other group all derive from methods which do correct for the presence of ligand on the sink side of the diffusion membrane. In addition, the isotherm extracted from the data obtained by the system transfer function method of analysis is seen to be comparable with the isotherm derived by the permeation constant method of analysis. However, because it is unnecessary to discard the data collected over the initial transient phase in the transfer function method of analysis, a greater number of data points, over a greater concentration range, are obtained for the same data set than by the permeation constant method. Thus, for an initial ligand concentration of 0.11×10^{-2} M, the upper concentration limit of the binding isotherm derived by the transfer function method of analysis is 0.76×10^{-3} M compared with an upper concentration limit of 0.60×10^{-3} M for the permeation constant method of analysis. There is, however, due to increased noise an increased level of uncertainty associated with this additional information. It should be noted that the additional points provided by the present transfer function method of analysis can represent a considerable portion of the isotherm because, although the data discarded during the initial transient phase in the permeation constant method represent only a small fraction of the total duration of the dialysis experiment, the points on the isotherm are not uniformly distributed in time. Moreover, the ligand concentration, and therefore the quantity of ligand bound to the protein, is greatest at the start of the dialysis.

From the point of view of mathematical rigour, the transfer function method is the preferred method of data analysis. The information content of each point in the elution profile depends on the signal-to-noise ratio. In the elution profile, the signal-to-noise

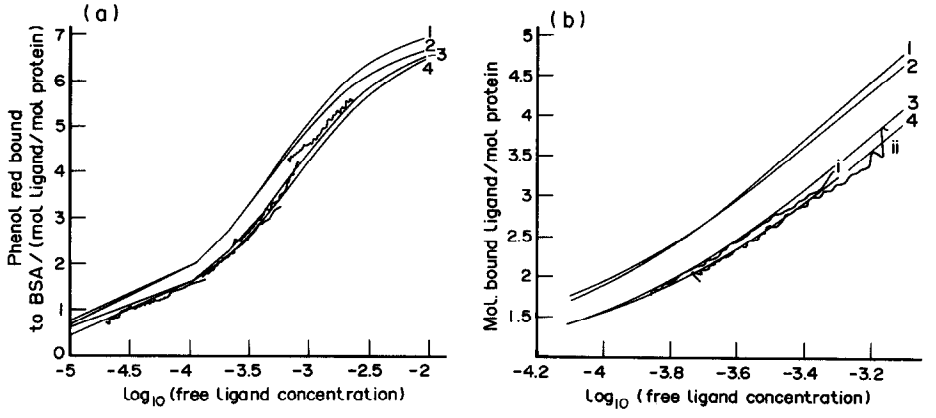

Figure 6
(a) Comparison of the Bjerrum plots of the phenol red–BSA binding isotherm obtained by the CFDD method (and calculated by the original permeation constant method [11]) with isotherms reported by other investigators. (b) Comparison of the binding isotherms obtained by the CFDD method using (i) the permeation constant method of analysis [11] and (ii) the present transfer function method. (1) Binding isotherm based on binding parameters of Kanfer [18]; (2) binding isotherm based on binding parameters of Meyer [3] and Guttman; (3) binding isotherm obtained by CFDD [11]; (4) binding isotherm based on binding parameters of Rodkey [15].

ratio decreases as the signal decreases. The permeation constant analysis evaluates the quantities $C_1^*(t)$ and $C_3^*(t)$ over the entire dialysis data set on the basis of a single average value of the permeation constant, irrespective of the signal-to-noise ratio. In the transfer function method of analysis, however, because of the Laplace transformation into the frequency domain the noise components of the signal are, in effect, averaged over the entire elution profile data set. The curves are smoothed by excluding those components which represent the high frequency noise.

References

[1] I. M. Klotz, F. M. Walker and R. B. Pivan, *J. Am. Chem. Soc.* **68**, 1486–1490 (1946).
[2] M. C. Meyer and D. E. Guttman, *J. Pharm. Sci.* **57**, 1627–1629 (1969).
[3] M. C. Meyer and D. E. Guttman, *J. Pharm. Sci.* **59**, 33–38 (1970).
[4] M. C. Meyer and D. E. Guttman, *J. Pharm. Sci.* **59**, 39–48 (1970).
[5] S. P. Colowick and F. C. Womack, *J. Biol. Chem.* **244**, 774–777 (1969).
[6] M. Lecureuil, B. Lejeune and G. Crouzat-Reynes, *J. Chim. Phys.* **70**, 782–788 (1973).
[7] J. S. Robertson and B. W. Madsen, *J. Pharm. Sci.* **63**, 234–239 (1974).
[8] D. Shieh, J. Feijen and D. J. Lyman, *Anal. Chem.* **47**, 1186–1187 (1975).
[9] E. Rachidy and S. Niazi, *J. Pharm. Sci.* **67**, 967–970 (1970).
[10] J. Fletcher, *J. Phys. Chem.* **81**, 2374–2378 (1977).
[11] N. A. Sparrow, A. E. Russell and L. Glasser, *Anal. Biochem.* **123**, 255–264 (1982).
[12] R. N. Bracewell, *The Fourier Transform and Its Applications*, 2nd Edn. McGraw-Hill, New York (1978).
[13] J. Greenberg, M.Sc. (Chem. Eng.) Dissertation. University of the Witwatersrand, Johannesburg, S.A. (1969).
[14] J. Wylie, *Advanced Engineering Mathematics*, 4th Edn. McGraw-Hill, New York (1975).
[15] F. L. Rodkey, *Archs Biochem. Biophys.* **94**, 38–47 (1969).
[16] C. Lanczos, *Applied Analysis*, pp. 225–229. Pitman, London (1967).
[17] L. V. Kantarovich and V. I. Krylov, *Approximate Methods in Higher Analysis*. Noordhof, Groningen (1964).
[18] I. Kanfer, Ph.D. Thesis, Rhodes University, Grahamstown, South Africa (1976).
[19] J. Chandler, *Quant. Chem. Program Exchange* **II**, 307 (1965).

[Received for review 22 November 1984; revised manuscript received 16 May 1985]